International Journal of Electrical, Electronic and Communication Sciences
ISSN: 2517-9438
Vol:10, No:10, 2016

Comparison of the Performance of GaInAsSb and GaSb Cells under Different Temperature Blackbody Radiations

Liangliang Tang, Chang Xu, Xingying Chen

***Abstract*—**GaInAsSb cells probably show better performance than GaSb cells in low-temperature thermophotovoltaic systems due to lower bandgap; however, few experiments proved this phenomenon so far. In this paper, numerical simulation is used to evaluate GaInAsSb and GaSb cells with similar structures under different radiation temperatures. We found that GaInAsSb cells with n-type emitters show slightly higher output power densities compared with that of GaSb cells with n-type emitters below 1,550 K-blackbody radiation, and the power density of the later cells will suppress the formers above this temperature point. During the temperature range of 1,000~2,000 K, the efficiencies of GaSb cells are about twice of GaInAsSb cells if perfect filters are used to prevent the emission of the non-absorbed long wavelength photons. Several parameters that affect the GaInAsSb cell were analyzed, such as doping profiles, thicknesses of GaInAsSb epitaxial layer and surface recombination velocity. The non-p junctions, i.e., n-type emitters are better for GaInAsSb cell fabrication, which is similar to that of GaSb cells.

***Keywords*—**Thermophotovoltaic cell, GaSb, GaInAsSb, diffused emitters.

I. Introduction

GaSb and GaInAsSb cells are both popular converters for thermophotovoltaic (TPV) systems. The bandgap of GaSb cell is 0.72 eV [1], and the GaInAsSb cell has the variable bandgap of 0.5~0.55 eV with the different design of elements match [2]-[5]. The GaInAsSb cell probably shows better output density than GaSb cell under lower radiation temperatures due to lower bandgap, thus it is necessary to compare their performance as a function of radiator temperatures, and this comparison will guide us to choose proper cells for different TPV systems.

The GaSb and GaInAsSb cells have been widely used in TPV systems using different radiators [6]-[9]; however, little work has been done on the investigation of their performance under the same radiator, with the exception of the group of Dr. Qiu [10]. They compared the output power density of GaSb and GaInAsSb cells using SiC radiators during the temperature range of 1173~1573 K. Unexpectedly, the GaSb cell showed better output density in lower temperatures, while the GaInAsSb cell showed better output density in higher temperatures. This experimental result may be contrary with theoretical condition because the GaInAsSb cell has the lower bandgap than that of the GaSb cell. Dr. Qiu explained that there may be some leakage current problems with the GaInAsSb cell which caused the abnormal phenomenon, the power density of GaInAsSb cell would be enhanced if the cell structure and manufacturing process were optimized.

Since no more comparison data can be obtained, it is valuable to make a theoretical calculation for evaluation of the performance of GaSb and GaInAsSb cells. In this paper, the performance of cells with four different structures (GaSb cells with p and n-type emitters, GaInAsSb cell with p and n-type emitters) are evaluated under different radiation spectrums. GaSb cells with Zn diffused p-emitters are the most developed [11], [12], thus all the diffused emitters are used for keep unity. The remainder of this paper is organized as follows. Section II provides the modeling of GaInAsSb cells with p and n-type emitters, from which we can obtain the optimal structure design of GaInAsSb cells, the modeling of GaSb cells is omitted and can be found in our previous work [13]. Section III evaluates the cell performance including the output power density and efficiency under different radiation spectrum. Section IV presents the comparison results and outlines the conclusions.

II. Modeling of GaInAsSb Cells with P and N-Type Diffused Emitters

The GaInAsSb cell with uniform doped emitter has been fabricated and simulated [2], [3], [5], [14]; a window layer should be deposited on the emitter to reduce the surface recombination velocity (*S*) [3]. If the p-n junction was formed by vapor diffusion, the window layer could be omitted due to the built-in electric fields formed by the gradient doped emitter [15]. Fig. 1 shows GaInAsSb cell structure with Zn-diffused p-emitters and the internal Zn profiles. The Zn profiles show the kink-and-tail (K&T) shapes in N-GaInAsSb [15], [16], the relationship between Zn diffusivity (D) and concentration (C) in N-GaInAsSb is similar to that in GaSb and GaAs [17], [18], i.e. $D \propto C^2$ for the region before the kink point and D□C for the tail region, the K&T profile, which was extracted from [15], and the respective simulation results are plotted in Fig. 1 (b). We found that Ga atoms in the diffusion source could suppress the formation of the surface D□C^2 region in both GaSb and GaAs [17], [18], thus we believe that the low-concentration $D \propto C$ tail region could be formed directly in GaInAsSb and no etching process was needed. The

Liangliang Tang is with the College of Energy and Electricity, Hohai University, Nanjing 210098, China (Corresponding author, phone: 0086-15195897736, e-mail: tangll@hhu.edu.cn).

D□C shaped Zn profiles are used for simulation in this paper, the second Zn diffusion process in [15] was not considered.

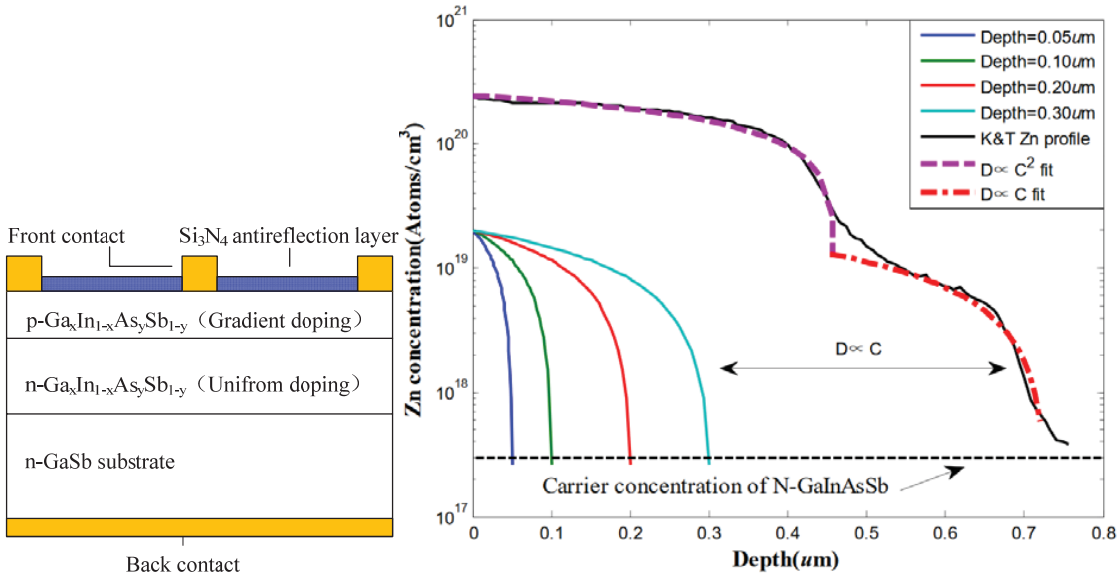

(a) Structure of GaInAsSb cells with Zn diffused p-emitters (b) Theoretical and experimental Zn profiles in the p-emitters

Fig. 1 (a) Structure of GaInAsSb cell with p-emitters, and (b) the internal Zn profiles

The element match of Ga: In: As: Sb = 0.84: 0.16: 0.14: 0.86 is chosen for the GaInAsSb cell, the relative bandgap is about 0.53e V. Table I shows the basic parameters of the GaInAsSb cells with p-type emitters used for simulation. A simple Si_3N_4 antireflective layer and 13.7% of grid area are used to keep unity with the GaSb cells [13]. The main carrier recombination mechanisms which affect the cell performances are the radiative, Auger, bulk Shokley-Read-Hall (SRH) and surface/interface recombination. The formulas and related parameters for simulating the recombination rates for GaInAsSb cells are summarized in Table II. The photon recycling factor (φ) is set at 4 because the back surface reflector (BSR) is not used; the value of S is set at 5 x $10^4 \sim 10^6$ cm/s for discussion and will be set at a high value of 10^6 cm/s for finial comparisons because no window layer is used; the above two settings are used to keep unity with the commercial Zn-diffused GaSb cells. The interface recombination velocity between GaSb substrate and GaInAsSb epitaxial layer is set at 1,500 cm/s.

Fig. 2 shows GaInAsSb cell structure with Te-diffused p-emitters and the internal Te profiles. There are no diffusion data to investigate the Te diffusion in GaInAsSb, thus the Te doping profiles which obey the complementary error function were approximately used for simulation, as shown in Fig. 2 (b). The carrier concentration of p-GaSb substrate and p-GaInAsSb epitaxial layer is 3×10^{17}cm^{-3}, the other parameters of n-on-p cells are similar to that p-on-n cells, as shown in Tables I and II.

TABLE I
BASIC PARAMETERS OF $GA_{0.84}IN_{0.16}AS_{0.14}SB_{0.86}$ CELLS WITH P-EMITTERS USED FOR SIMULATION

Basic parameters	Numerical value
Intrinsic carrier concentration n_i, at 300K	4.5×10^{13}cm^{-3}[5]
Absorption coefficient of $Ga_{0.84}In_{0.16}As_{0.14}Sb_{0.86}$	Extracted from [13]
Antireflection layer: Si_3N_4 layer	0.20μm
Grid area/Surface area	13.7%
Thickness of N-GaSb substrate	400μm
Carrier concentration of N-GaSb substrate	3×10^{17}cm^{-3}
Thickness of N-$Ga_{0.84}In_{0.16}As_{0.14}Sb_{0.86}$ epitaxial layer	3 ~ 6μm
N- $Ga_{0.84}In_{0.16}As_{0.14}Sb_{0.86}$ doping: Te doping	3×10^{17}cm^{-3}
P-type emitter: Zn doping	Zn profile shown in Fig. 1 (b)
Electron mobility in $Ga_{0.84}In_{0.16}As_{0.14}Sb_{0.86}$ $\mu=\mu_{min}+\frac{\mu_{max}-\mu_{min}}{1+((N_D+N_A)/N_{ref})^{\alpha}}$	$\mu_{max}=8500$cm^2/V·s [5] $\mu_{min}=420$cm^2/V·s $N_{ref}=5\times10^{17}$cm^{-3} $\alpha=0.7$
Hole mobility in $Ga_{0.84}In_{0.16}As_{0.14}Sb_{0.86}$ $\mu=\mu_{min}+\frac{\mu_{max}-\mu_{min}}{1+((N_D+N_A)/N_{ref})^{\alpha}}$	$\mu_{max}=500$cm^2/V·s [5] $\mu_{min}=110$cm^2/V·s $N_{ref}=9\times10^{17}$cm^{-3} $\alpha=0.66$

The GaInAsSb cell is simulated using 1-D numerical photovoltaic cell simulation program PC-1D [20], which solves the fully coupled nonlinear equations for the transport of electrons and holes. Variable radiation spectra can be defined by users in PC1D, thus this simulation program can be extended to evaluate the performance of radiation materials

and filters in TPV systems. The parameters, such as diffusion depth, thickness of GaInAsSb epitaxial layer and *S* value which affect the cell performance will be discussed firstly in order to choose the optimal parameters for the GaInAsSb cell.

A. Effect of the Diffusion Depth on Cell Performance

The gradient Zn or Te doping could be formed by vapor diffusion, and the internal quantum efficiency (IQE) of the GaInAsSb cell could keep a considerable value without a window layer to reduce the *S* value. In this condition, the *S* value is set at 10^6 cm/s and the thickness of the N or P-GaInAsSb epitaxial layer is 5 μm in this simulation process. Fig. 3 shows the IQE of the GaInAsSb cells with p and n-type emitters using different diffusion depth. Both the IQE data decrease with the increasing of diffusion depth, thus light doping is better for cell design and the depth of 0.1 μm will be chosen for both cells in the following simulations. The GaInAsSb cells with n-emitters show better IQE than of the cells with p-emitters in the long wavelengths region.

TABLE II
SUMMARY OF RECOMBINATION PARAMETERS FOR $GA_{0.84}IN_{0.16}AS_{0.14}SB_{0.86}$ AT 300 K

Recombination	Recombination rates	Parameters
Radiative	$R_{Rad}=\frac{B}{\varphi}(np-n_i^2)$	$B=1\times10^{-10}\,\mathrm{cm}^3/\mathrm{s}$ [5] $\varphi=4$
Auger	$R_{Aug}=(C_n+C_p p)(np-n_i^2)$	$C_p=C_n=2\times10^{-28}\,\mathrm{cm}^6/\mathrm{s}$ [5]
Bulk SRH	$R_{SRH}=\frac{(np-n_i^2)}{\tau_{SRHe}(p+n_i)+\tau_{SRHh}(n+n_i)}$	$\tau_{SRHe}=\tau_{SRHe}=120\mathrm{ns}$ [19]
Surface/Interface	$R_{Sur/Inter}=\frac{S_e S_h(np-n_i^2)}{S_e(p+n_i)+S_h(n+n_i)}$	Surface: $S_e=S_h=5\times10^4\sim10^6\,\mathrm{cm/s}$ Interface:$S_e=S_h=1500\mathrm{cm/s}$

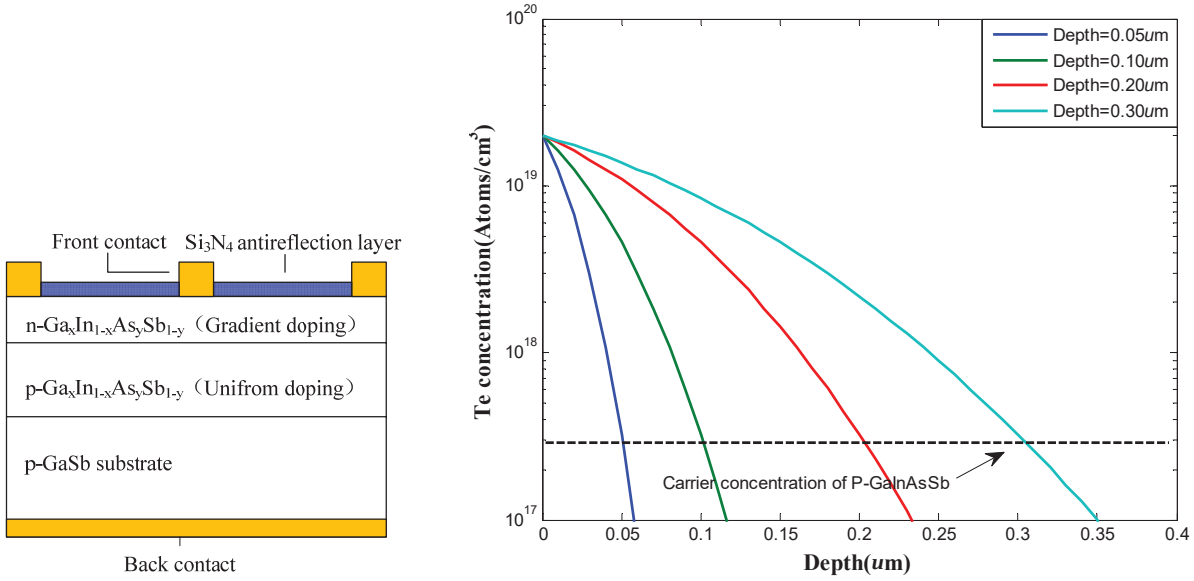

(a) Structure of GaInAsSb cells with Te diffused n-emitters (b) ERFC Te profiles in the n-emitters

Fig. 2 (a) Structure of GaInAsSb cell with n-emitters, and (b) the internal ERFC-Te profiles

B. Effect of the Thickness of GaInAsSb Epitaxial Layer on Cell Performance

The base region of GaInAsSb cells contributes the largest part of IQE in the long wavelength. Photo-generated minority carriers would not be fully collected if the base region was too thin. Conversely, minority carrier pairs would recombine if the base region was too thick. Fig. 4 shows the IQE of the GaInAsSb cells with p and n-type emitters using different thickness of the GaInAsSb epitaxial layer, the diffusion depth is 0.1 μm and the *S* value is set at 10^6 cm/s. As for the cells with p-emitters, the IQE will decrease before 1700 nm and increase after this wavelength along with the deepening of the N-GaInAsSb epitaxial layer. As for the cells with n-emitters, the IQE will keep constant before 1700 nm and increase after this wavelength along with the deepening of the P-GaInAsSb epitaxial layer. The above different variation tendency may be caused by the different diffusion depth between holes and electrons in GaInAsSb layers.

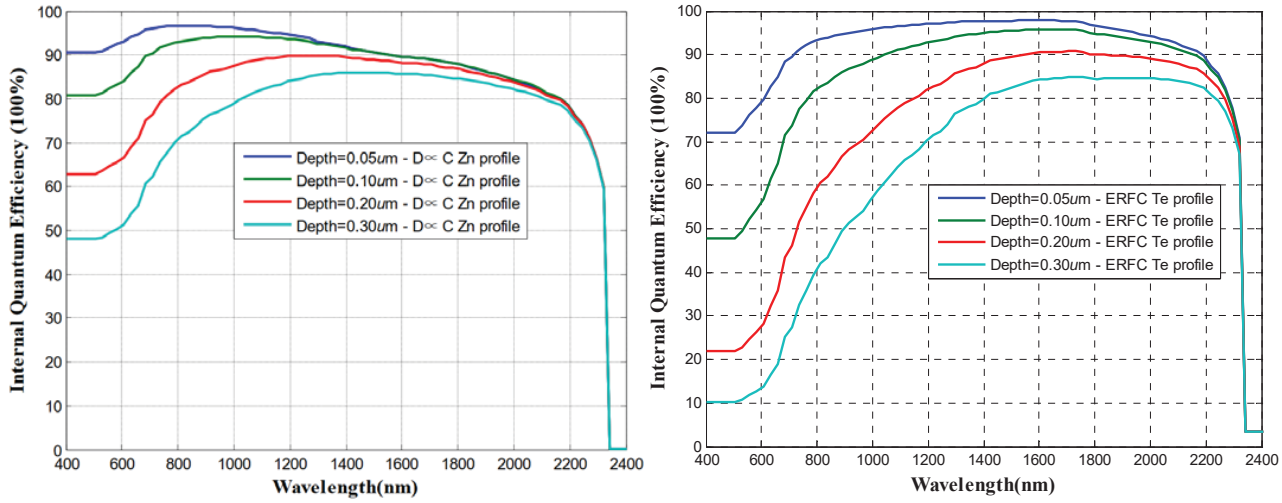

(a) (b)

Fig. 3 (a) IQE of the GaInAsSb cells with p-type emitters, and (b) n-type emitters using different diffusion depth

C. Effect of the Surface Recombination Velocity on Cell Performance

The average IQE of GaInAsSb cells with uniform doped emitters will decrease rapidly if the *S* value surpasses 10^5 cm/s [14], thus a window layer would be needed to reduce the *S* value; while the high *S* value will not affect the IQE heavily if gradient doped emitters are used. Fig. 5 shows the calculated IQE of the GaInAsSb cells with p and n-type emitters using different *S* values. The thickness of N or P-GaInAsSb epitaxial layer is 5 μm and the diffusion depth is 0.1 μm in this simulation process. The IQE of both cells only decrease in the short wavelength, thus the cell performance will not decrease rapidly.

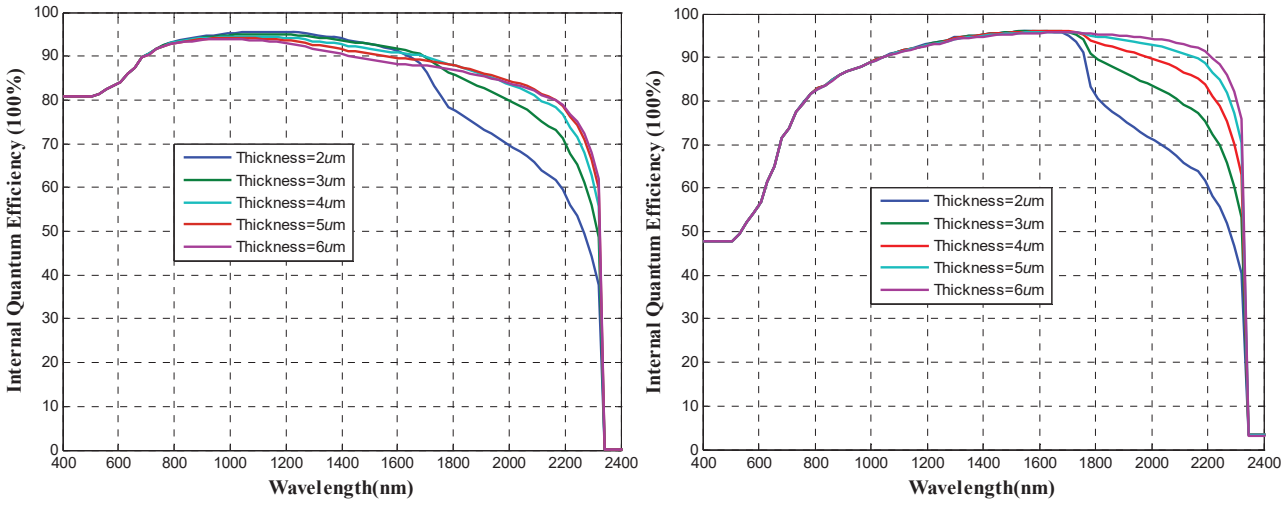

(a) (b)

Fig. 4 (a) IQE of the GaInAsSb cells with p-type emitters, and (b) n-type emitters using different thickness of GaInAsSb epitaxial layer

III. Evaluation the Cell Performance under Different Radiation Spectrum

The short-circuit current (I_{sc}) of GaInAsSb cells will be larger than that of GaSb cells; however, the open circuit voltage (V_{oc}) and fill factor (FF) of the former cell will decrease due to the low bandgap. The cell parameter of I_{sc}, V_{oc} and FF should be considered overall, the output power density and cell efficiency are the ultimate indicators for performance check. In this section, the optimal cell structure will be chosen for their evaluation performances under 1,000~2,000 K-blackbody radiation, useful comparison results will be obtained.

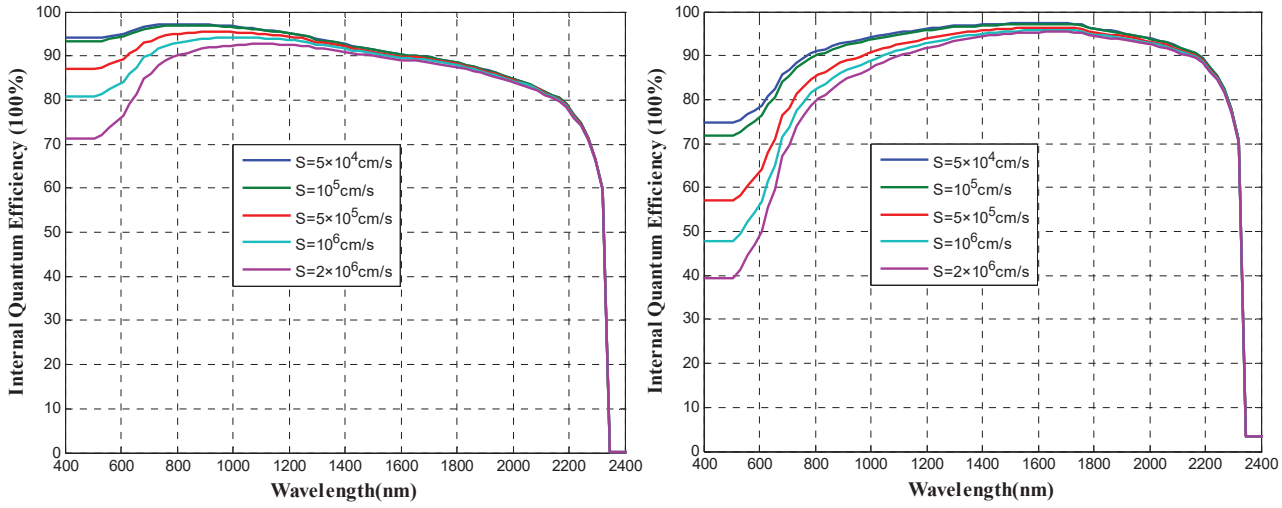

(a) (b)

Fig. 5 (a) IQE of the GaInAsSb cells with p-type emitters, and (b) n-type emitters using different *S* values

A. Selection of the GaInAsSb and GaSb Cell Structure for Performance Evaluation

Fig. 6 shows IQE, external quantum efficiency (EQE), and reflectivity (REF) of the GaInAsSb with p and n-emitters used for comparison. The diffusion depth is 0.1 μm and the *S* value is 10^6 cm/s for both the p-on-n or inverted structures. The gird area percent is set at 13.7% for keep unity with that of the GaSb cell. The antireflection (ARC) layer of the Zn-diffused GaInAsSb fabricated by Frounhofer is 0.136 μm thick anodic oxide (refractive index n≈2). The 0.136 μm ARC layer maybe too thin for the GaInAsSb cells and the minimum REF value locates at 1.2 μm [15], thus we choose the 0.20 μm Si_3N_4 (n≈2) ARC layer for the GaInAsSb cells. The thickness of the N-GaInAsSb epitaxial layer for the p-on-n structure is set at 5 μm, the IQE before 1,700 nm will decrease with the deepening of the N-GaInAsSb layer. The thickness of the P-GaInAsSb epitaxial layer for p-on-n structure is set at 6 μm, the IQE will increase with the deepening of P-GaInAsSb layer, the thickness of 6 μm is chosen for considering the cost of the epitaxial process.

The IQE of GaInAsSb cells with n-type emitters is higher than that of cells with p-type emitters in the long wavelength region; this phenomenon is caused by the disparities between the diffusion length of electrons and holes in GaInAsSb. The GaInAsSb cells with n-type emitters will show better output power density in TPV systems than that of p-type emitters, which are similar to GaSb cells.

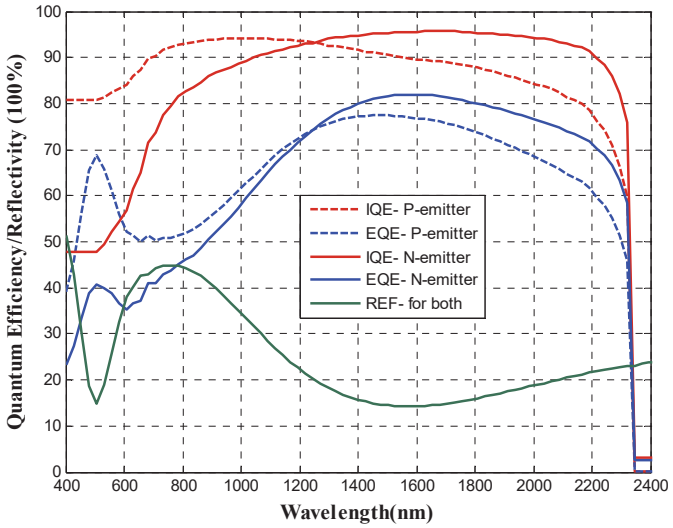

Fig. 6 IQE, EQE, and REF of the GaInAsSb cells with p and n-type emitters used for comparison

Fig. 7 shows the IQE, EQE, and REF of the GaSb cells with p and n-type emitters used for comparison. The diffusion depth, grid area percent, and *S* are set at the same value as that in the GaInAsSb cells. The specific parameters for simulation

in the GaSb cells could be found in our previous work [13]. The I_{sc} of GaSb cell would smaller than that of the GaInAsSb cell due to its narrow EQE data.

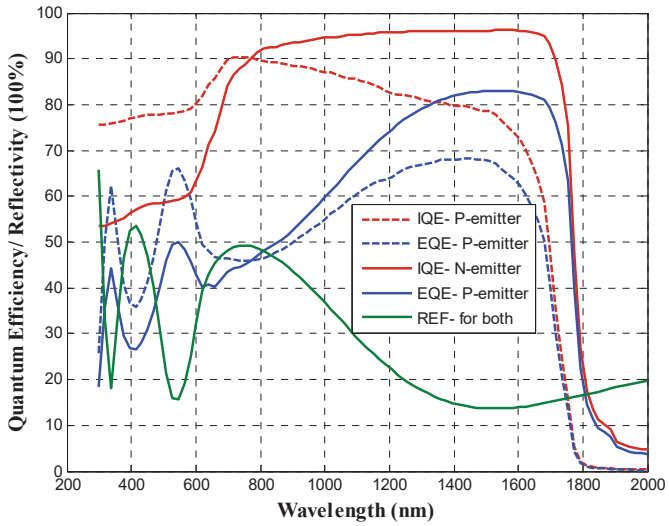

Fig. 7 IQE, EQE, and REF of the GaSb cells with p and n-type emitters used for comparison

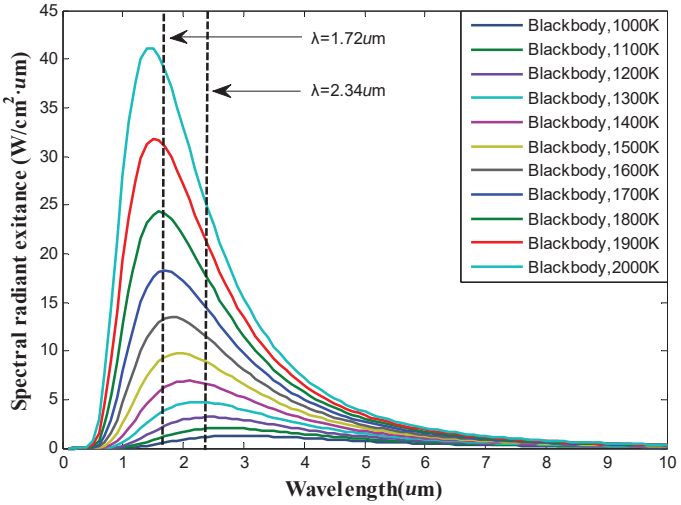

Fig. 8 Spectrum distributions of 1,000~2,000 K-blackbody radiation

B. The Cell Performance under 1,000~2,000 K-Blackbody Radiation with No Filters

Fig. 8 shows the spectrum distributions of 1,000~2,000 K-blackbody radiation. Two dashed lines in Fig. 8 demonstrate the cut-off wavelengths for GaSb and GaInAsSb cells, the left 1.72 μm for 0.72eV-GaSb cells and the right 2.34 μm for 0.53eV-GaInAsSb cells. The power densities within the cut-off wavelength of GaInAsSb cells are much larger than that of the GaSb cells during the temperature range of 1,000~2,000 K.

The I_{sc}, V_{oc} and FF of four types of TPV cells under 1,000~2,000 K-blackbody radiation are shown in Fig. 9. The I_{sc} of GaInAsSb cells are much larger than GaSb cells during the complete temperature range, while the V_{oc} and FF of the former cells are lower than that of the later cells. By multiplying the above three parameters, the maximum output power density (P_{max}) could be obtained, as shown in Fig. 10. The P_{max} of GaInAsSb cells with n-type emitters are larger than that of p-type emitters during the temperature range of 1,000~2,000 K. The P_{max} of GaSb cells with n-type emitters are larger than that of p-type emitters during the temperature range of 1,000~1,800 K, the comparison results will reverse after 1,800 K due to the superior FF of GaSb cells with p-emitters.

GaInAsSb cells with n-type emitters show slightly higher P_{max} compared with that of GaSb cells with n-type emitters below 1,550 K-blackbody radiation, and the P_{max} of the later cell will suppress the former above this temperature point. The GaInAsSb cells with p-type emitters show higher P_{max} compared with that of GaSb cells with p-type emitters below

1,820 K-blackbody radiation, the differences of P_{max} are considerable, the comparison results will reverse after 1,820 K. The tendencies of the cell efficiencies under pure blackbody radiation are similar to that of P_{max}, as shown in Fig. 10.

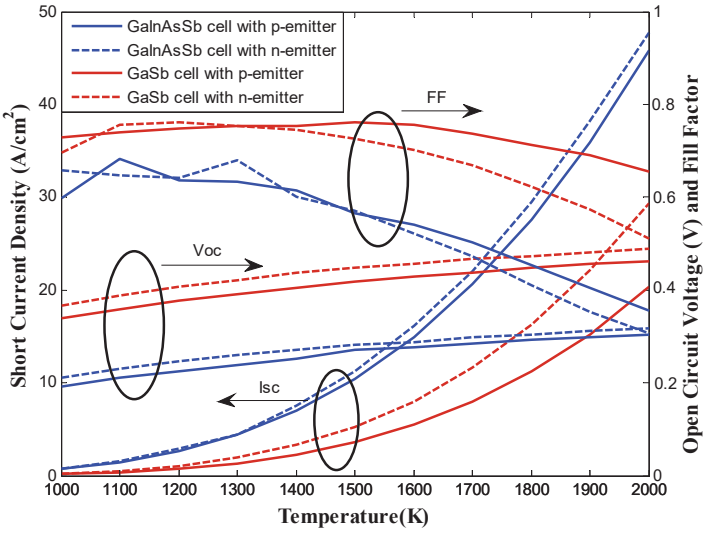

Fig. 9 The Isc, Voc, and FF of different TPV cells under 1,000~2,000 K-blackbody radiation

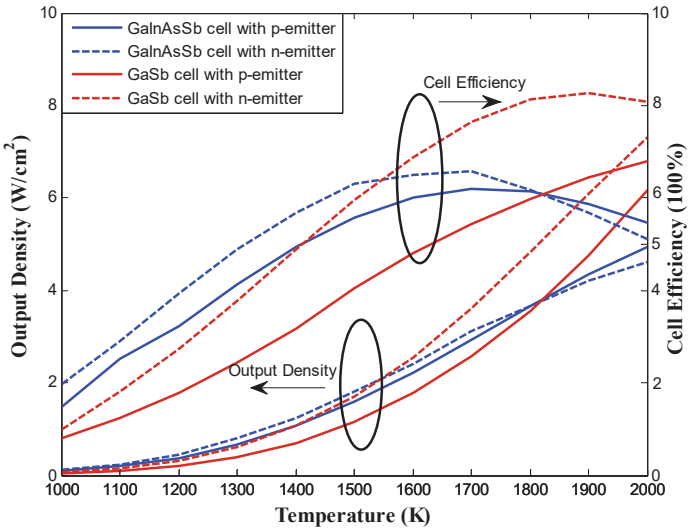

Fig. 10 Output power density and efficiency of different TPV cells under 1,000~2,000 K-blackbody radiation with no filters

C. The Cell Performance under 1,000~2,000 K-Blackbody Radiation with Perfect Filters

Optical filters were commonly used in TPV systems to prevent the emission of non-absorbed photons, and the cell efficiencies will enhance greatly if efficient filters were used. Fig. 11 shows the output power density and cell efficiency under 1,000~2,000 K-blackbody radiation with perfect filters. The perfect filters have the function that the non-absorbed photons ($\lambda \geq 1.72\mu$m for GaSb and $\lambda \geq 2.34\mu$m for GaInAsSb) were all prevented to transmit to the cell surface. The output power densities of the four cells are same to that in Fig. 10, while the cell efficiencies change substantially. The GaSb cell with n-type emitters shows the best efficiency among the four cells, and its efficiency is about twice that compared with GaInAsSb cells during the temperature range of 1,000~2,000 K.

IV. Conclusion

The GaInAsSb cells with diffused emitters were analyzed in this paper, and the n-on-p structures show the better performance than that of p-on-n structures. The V_{oc} of GaInAsSb cells reached about 300 mV without the window layer due to the built-in electrical field caused by gradient doping. The performance of GaInAsSb and GaSb cells were evaluated under 1,000~2,000 K-blackbody radiation with no and perfect filters. We found that GaInAsSb cells with n-type emitters show slightly higher P_{max} compared with that of GaSb cells with n-type emitters below 1,550 K-blackbody radiation,

and the P_{max} of the later cells will surpass the formers above this temperature point. The GaInAsSb cells with p-type emitters showed higher P_{max} compared with that of GaSb cells with p-type emitters below 1,820 K-blackbody radiation, the comparison results will reverse after 1,820 K. The GaSb cells showed twice the efficiencies compared with GaInAsSb cells during the temperature range of 1,000~2,000 K if the perfect filter were used.

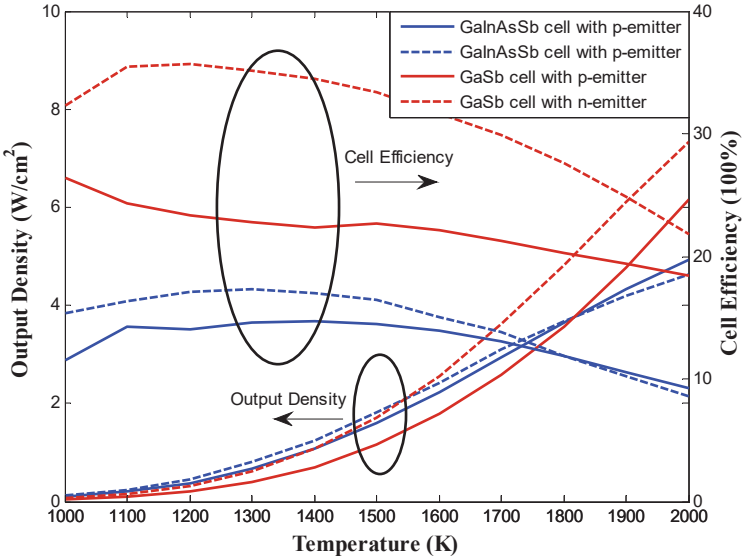

Fig. 11 Output power density and efficiency of different TPV cells under 1,000~2,000 K-blackbody radiation with perfect filters

ACKNOWLEDGMENT

This work was supported by the National Natural Science Foundation of China (No. 51506045) and Natural Science Foundation of Jiang Su (No. BK20150805). The authors wish to thank Dr. Lewis M. Fraas (President of JX Crystals Inc.) and Jany Fraas for their original idea about III-V-based TPV cells with n-type emitters. The authors are also grateful to the University of New South Wales, for their free-shared PC-1D program.

REFERENCES

[1] L.M. Fraas, G.R. Girard, J.E. Avery, B.A. Arau, V.S. Sundaram, A.G. Thompson, J.M. Gee, Gasb Booster Cells for over 30-Percent Efficient Solar-Cell Stacks, J Appl Phys, 66 (1989) 3866-3870.

[2] C. Wang, H. Choi, S. Ransom, G. Charache, L. Danielson, D. DePoy, High-quantum-efficiency 0.5 eV GaInAsSb/GaSb thermophotovoltaic devices, Applied physics letters, 75 (1999) 1305-1307.

[3] H. Choi, C. Wang, G. Turner, M. Manfra, D. Spears, G. Charache, L. Danielson, D. Depoy, High-performance GaInAsSb thermophotovoltaic devices with an AlGaAsSb window, Applied physics letters, 71 (1997) 3758-3760.

[4] R. Magri, A. Zunger, H. Kroemer, Evolution of the band-gap and band-edge energies of the lattice-matched GaInAsSb/ GaSb and GaInAsSb/ InAs alloys as a function of composition, Journal of applied physics, 98 (2005) 043701.

[5] M.W. Dashiell, J.F. Beausang, H. Ehsani, G. Nichols, D.M. Depoy, L.R. Danielson, P. Talamo, K.D. Rahner, E.J. Brown, S.R. Burger, Quaternary InGaAsSb thermophotovoltaic diodes, Electron Devices, IEEE Transactions on, 53 (2006) 2879-2891.

[6] L.M. Fraas, J.E. Avery, H.X. Huang, Thermophotovoltaic furnace-generator for the home using low bandgap GaSb cells, Semicond Sci Tech, 18 (2003) S247-S253.

[7] A.W. Bett, O.V. Sulima, GaSb photovoltaic cells for applications in TPV generators, Semicond Sci Tech, 18 (2003) S184-S190.

[8] K. Qiu, A. Hayden, Direct thermal to electrical energy conversion using very low bandgap TPV cells in a gas-fired furnace system, Energy Conversion and Management, 79 (2014) 54-58.

[9] W.R. Chan, P. Bermel, R.C. Pilawa-Podgurski, C.H. Marton, K.F. Jensen, J.J. Senkevich, J.D. Joannopoulos, M. Soljačić, I. Celanovic, Toward high-energy-density, high-efficiency, and moderate-temperature chip-scale thermophotovoltaics, Proceedings of the National Academy of Sciences, 110 (2013) 5309-5314.

[10] K. Qiu, A. Hayden, M. Mauk, O. Sulima, Generation of electricity using InGaAsSb and GaSb TPV cells in combustion-driven radiant sources, Solar energy materials and solar cells, 90 (2006) 68-81.

[11] L.M. Fraas, J.E. Avery, G. Girard, G.R. Girard, Tandem Photovoltaic Solar Cell with III-V Diffused Junction Booster Cell, in, Boeing Co (Boei), US patent,1992.

[12] L.M. Fraas, V.S. Sundaram, J.E. Avery, P.E. Gruenhaum, E. Malocsay, III-V Solar Cells and Doping Progresses, in, Boeing Co (Boei), US patent 1993.

[13] L. Tang, L.M. Fraas, Z. Liu, C. Xu, X. Chen, Performance Improvement of the GaSb Thermophotovoltaic Cells with n-Type Emitters, IEEE transactions on electron devices, 62 (2015) 2809-2815.

[14] X. Peng, X. Guo, B. Zhang, X. Li, X. Zhao, X. Dong, W. Zheng, G. Du, Numerical analysis of the short-circuit current density in GaInAsSb thermophotovoltaic diodes, Infrared Physics & Technology, 52 (2009) 152-157.

[15] O. Sulima, R. Beckert, A. Bett, J. Cox, M. Mauk, InGaAsSb photovoltaic cells with enhanced open-circuit voltage, IEE Proceedings-Optoelectronics, 147 (2000) 199-204.

[16] O.V. Sulima, A.W. Bett, M.G. Mauk, B.Y. Ber, P.S. Dutta, Diffusion of Zn in TPV materials: GaSb, InGaSb, InGaAsSb and InAsSbP. In: Thermophotovoltaic Generation of Electricity, in: Thermophotovoltaic Generation of Electricity: Fifth Conference on Thermophotovoltaic Generation of Electricity, 2003, pp. 402-413.

[17] H. Ye, L. Tang, K. Li, The intrinsic relationship between the kink-and-tail and box-shaped zinc diffusion profiles in n-GaSb, Semiconductor Science and Technology, 28 (2013) 015001.

[18] H. Ye, L. Tang, Q. Ni, Identification of the dissociative and kick-out diffusion mechanisms of Zn diffusion in GaAs by photoluminescence analysis, Materials Science & Engineering B, 197 (2015) 1-4.

[19] Y. Wang, N. Chen, X. Zhang, T. Huang, Z. Yin, Y. Wang, H. Zhang, Evaluation of thermal radiation dependent performance of GaSb

thermophotovoltaic cell based on an analytical absorption coefficient model, Solar Energy Materials and Solar Cells, 94 (2010) 1704-1710.
[20] D.A. Clugston, P.A. Basore, PC1D version 5: 32-bit solar cell modeling on personal computers, in: Photovoltaic Specialists Conference, 1997., Conference Record of the Twenty-Sixth IEEE, IEEE, 1997, pp. 207-210.